

## Hyperspectral Fluorescence and Reflectance Imaging Instrument

**A single system contains spatial-scanning, illumination, and spectral-imaging subsystems.**

*Stennis Space Center, Mississippi*

The system is a single hyperspectral imaging instrument that has the unique capability to acquire both fluorescence and reflectance high-spatial-resolution data that is inherently spatially and spectrally registered. Potential uses of this instrument include plant stress monitoring, counterfeit document detection, biomedical imaging, forensic imaging, and general materials identification.

Until now, reflectance and fluorescence spectral imaging have been performed by separate instruments. Neither a reflectance spectral image nor a fluorescence spectral image alone yields as much information about a target surface as does a combination of the two modalities. Before this system was developed, to benefit from this combination, analysts needed to perform time-consuming post-processing efforts to co-register the reflective and fluorescence information. With this instrument, the inherent spatial and spectral registration of the reflectance and fluorescence images minimizes the need for this post-processing step.

The main challenge for this technology is to detect the fluorescence signal in the presence of a much stronger reflectance signal. To meet this challenge, the instrument modulates artificial light sources from ultraviolet through the visible to the near-infrared part of the spectrum; in this way, both the reflective and

fluorescence signals can be measured through differencing processes to optimize fluorescence and reflectance spectra as needed.

The main functional components of the instrument are a hyperspectral imager, an illumination system, and an image-plane scanner. The hyperspectral imager is a one-dimensional (line) imaging spectrometer that includes a spectrally dispersive element and a two-dimensional focal plane detector array. The spectral range of the current imaging spectrometer is between 400 to 1,000 nm, and the wavelength resolution is approximately 3 nm. The illumination system consists of narrowband blue, ultraviolet, and other discrete wavelength light-emitting-diode (LED) sources and white-light LED sources designed to produce consistently spatially stable light. White LEDs provide illumination for the measurement of reflectance spectra, while narrowband blue and UV LEDs are used to excite fluorescence. Each spectral type of LED can be turned on or off depending on the specific remote-sensing process being performed. Uniformity of illumination is achieved by using an array of LEDs and/or an integrating sphere or other diffusing surface. The image plane scanner uses a fore optic with a field of view large enough to provide an entire scan line on the image plane. It builds up a two-dimensional image in

pushbroom fashion as the target is scanned across the image plane either by moving the object or moving the fore optic.

For fluorescence detection, spectral filtering of a narrowband light illumination source is sometimes necessary to minimize the interference of the source spectrum wings with the fluorescence signal. Spectral filtering is achieved with optical interference filters and absorption glasses. This dual spectral imaging capability will enable the optimization of reflective, fluorescence, and fused datasets as well as a cost-effective design for multispectral imaging solutions. This system has been used in plant stress detection studies and in currency analysis.

*This work was done by Robert E. Ryan and S. Duane O'Neal of Science Systems and Applications, Inc.; Mark Lanoue of the Institute for Technology Development; and Jeffrey Russell of Computer Sciences Corporation for Stennis Space Center.*

*Inquiries concerning rights for its commercial use should be addressed to:*

*Institute For Technology Development  
Stennis Space Center  
Bldg. 1103, Suite 118  
Stennis Space Center, MS 39529  
E-mail: Mark.Lanoue@iftd.org  
Phone No.: (228) 688-2509*

*Refer to SSC-00254, volume and number of this NASA Tech Briefs issue, and the page number.*

## Improving the Optical Quality Factor of the WGM Resonator

**New iterative annealing and polishing increases the resonator's finesse over the fundamental limit.**

*NASA's Jet Propulsion Laboratory, Pasadena, California*

Resonators usually are characterized with two partially dependent values: finesse ( $\mathcal{F}$ ) and quality factor ( $Q$ ). The finesse of an empty Fabry-Perot (FP) resonator is defined solely by the quality of its mirrors and is calculated as

$$\mathcal{F} = \pi R^{1/2} / (1 - R).$$

The maximum up-to-date value of reflectivity  $R \approx 1 - 1.6 \times 10^{-6}$  is achieved with dielectric mirrors. An FP resonator made with the mirrors has finesse  $\mathcal{F} = 1.9 \times 10^6$ . Further practical increase of the finesse of

FP resonators is problematic because of the absorption and the scattering of light in the mirror material through fundamental limit on the reflection losses given by the internal material losses and by thermodynamic density fluctuations on the order of parts in  $10^9$ . The quality factor of a resonator depends on both its finesse and its geometrical size. A one-dimensional FP resonator has  $Q = 2 \mathcal{F} L / \lambda$ , where  $L$  is the distance between the mirrors and  $\lambda$  is the wavelength. It is easy to see that the quality fac-

tor of the resonator is unlimited because  $L$  is unlimited.  $\mathcal{F}$  and  $Q$  are equally important.

In some cases, finesse is technically more valuable than the quality factor. For instance, buildup of the optical power inside the resonator, as well as the Purcell factor, is proportional to finesse. Sometimes, however, the quality factor is more valuable. For example, inverse threshold power of intracavity hyperparametric oscillation is proportional to  $Q^2$  and efficiency of parametric fre-

quency mixing is proportional to  $Q^2$ . Therefore, it is important to know both the maximally achievable finesse and quality factor values of a resonator.

Whispering gallery mode (WGM) resonators are capable of achieving larger finesse compared to FP resonators. For instance, fused silica resonators with finesse  $2.3 \times 10^6$  and  $2.8 \times 10^6$  have been demonstrated. Crystalline WGM resonators reveal even larger finesse values,  $\mathcal{F} = 6.3 \times 10^6$ , because of low attenuation of light in the transparent optical crystals. The larger values of  $\mathcal{F}$  and  $Q$  result in the enhancement of various nonlinear processes. Low-threshold Raman lasing, optomechanical oscillations, frequency doubling, and hyper-

parametric oscillations based on these resonators have been recently demonstrated. Theory predicts a possibility of nearly  $10^{14}$  room-temperature optical  $Q$ -factors of optical crystalline WGM resonators, which correspond to finesse levels higher than  $10^9$ . Experiments have shown numbers a thousand times lower than that. The difference occurs due to media imperfections.

To substantially reduce the optical losses caused by the imperfections, a specific, multi-step, asymptotic processing of the resonator is implemented. The technique has been initially developed to reduce microwave absorption in dielectric resonators. One step of the process consists of mechanical polishing

performed after high temperature annealing. Several steps repeat one after another to lead to significant reduction in optical attenuation and, as a result, to the increase of  $Q$ -factor as well as finesse of the resonator which demonstrates a  $\text{CaF}_2$  WGM resonator with  $\mathcal{F} > 10^7$  and  $Q > 10^{11}$ .

*This work was done by Lute Maleki of OE Waves and Anatoliy Savchenkov, Andrey Matsko, and Vladimir Ilchenko of Caltech for NASA's Jet Propulsion Laboratory.*

*This invention is owned by NASA, and a patent application has been filed. Inquiries concerning nonexclusive or exclusive license for its commercial development should be addressed to the Patent Counsel, NASA Management Office-JPL. Refer to NPO-45053.*

## Ultra-Stable Beacon Source for Laboratory Testing of Optical Tracking

**A prototype laser beacon assembly provides reference for testing tracking and pointing systems.**

*NASA's Jet Propulsion Laboratory, Pasadena, California*

The ultra-stable beacon source (USBS) provides a laser-beam output with a very low angular jitter and can be used as an absolute angular reference to simulate a beacon in the laboratory. The laser is mounted on the top of a very short ( $\approx 1$  m) inverted pendulum (IP) with its optical axis parallel to the carbon fiber pendulum leg. The 85-cm, carbon fiber rods making up the leg are very lightweight and rigid, and are supported by a flex-joint at the bottom (see figure). The gimbal-mounted laser is a weight-adjustable load of about 1.5 kg with its center of rotation co-located with the center of percussion of the inverted pendulum. This reduces the coupling of transverse motion at the base of the pendulum to angular motion of the laser at the top.

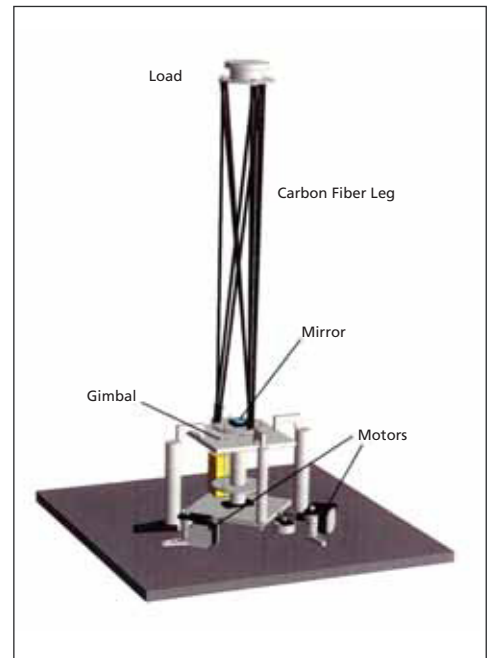
The inverted pendulum is mounted on a gimbal with its center of rotation coinciding with the pivot position of the inverted pendulum flexure joint. This reduces coupling of ground tilt at the inverted pendulum base to motion of the laser mounted at the top. The mass of the top gimbal is adjusted to give the pendulum a very low resonant frequency ( $\approx 10$  mHz) that filters transverse seismic disturbances from the ground where the base is attached.

The motion of the IP is monitored by an optical-lever sensor. The laser light is reflected by the mirror on the IP, and

then is detected by a quadrant photo-detector (QPD). The position of the beam spot on the QPD corresponds to the tilt of the IP. Damping of this motion is provided by two coil and magnet pairs.

The bottom gimbal mount consists of two plates. The IP is mounted on the second plate. The first plate is supported by two posts through needles and can be rotated about the axis connecting the tips of the needles. The second plate hangs from the first plate and can be rotated about the axis perpendicular to the first plate. As a result, the second plate acts as a two-axis rotation stage. Its center of rotation is located at the effective bending point of the flex-joint. The second plate is pressed against two screw actuators by the weight of the IP. The screw actuators are orthogonal to each other and are used to adjust the inclination of the second plate. The actuators are driven by stepper motors.

The whole IP system is housed in a box made of Lexan plastic plates to provide isolation from air currents and temperature variations. The signals from the sensors are processed and recorded with a PC using the xPC Target realtime environment of MathWorks. The control algorithms are writ-



In the **Inverted Pendulum** configuration, an additional gimbal is mounted at the top with a laser at the center of rotation. The laser provides the outgoing beacon source.

ten using the Simulink package from The MathWorks.

*This work was done by Yoichi Aso and Szabolcs Marka of Columbia University and Joseph Kovalik of Caltech for NASA's Jet Propulsion Laboratory. Further information is contained in a TSP (see page 1). NPO-45127.*